

Development of GIS toolbar to estimate reference evapotranspiration and net irrigation requirement on raster based approach

Minotshing Maza¹, Arnab Bandyopadhyay^{2*}, Aditi Bhadra³

(1. Assistant Engineer, O/o Chief Engineer (Planning & Design), Water Resources Department, Chimpu, Itanagar – 791113, Arunachal Pradesh;

2. Associate Professor, Department of Agricultural Engineering, North Eastern Regional Institute of Science and Technology, Nirjuli (Itanagar) – 791109, Arunachal Pradesh;

3. Associate Professor, Department of Agricultural Engineering, North Eastern Regional Institute of Science and Technology, Nirjuli (Itanagar) – 791109, Arunachal Pradesh)

Abstract: An ArcGIS toolbar was developed with the help of ArcObjects within ArcGIS environment to estimate evapotranspiration (ET) and net irrigation requirement (NIR) on raster based approach. The toolbar can estimate ET on a daily or monthly basis either with Hargreaves and Samani method or FAO56-PM method and calculate the corresponding NIR on a monthly basis. The toolbar was tested using normal monthly meteorological data (maximum temperature, minimum temperature, relative humidity, wind speed, solar radiation and rainfall) collected from 133 India Meteorological Department (IMD) stations covering 19 agro-ecological regions from 1971–2000. These point meteorological data were interpolated using ordinary kriging method and resampled at 1 km spatial resolution to generate the input rasters. Crop coefficient (k_c) raster for each month was prepared by analysing the cropping pattern of the country. Using the developed toolbar, reference evapotranspiration (ET_o) was estimated using both the methods on a monthly basis and NIR was estimated using the ET_o of FAO56-PM method and comparison was made between the two ET_o estimates. Verification of ET_o and NIR estimates made by the toolbar was performed by comparing the toolbar estimated monthly ET_o and NIR with manually calculated ones at ten evenly distributed locations and was found that the toolbar can generate accurate ET_o and NIR rasters.

Keywords: evapotranspiration, net irrigation requirement, ArcObjects, raster, FAO-56 PM, Hargreaves and Samani

Citation: Maza, M., A. Bandyopadhyay, and A. Bhadra. 2020. Development of GIS toolbar to estimate reference evapotranspiration and net irrigation requirement on raster based approach. *Agricultural Engineering International: CIGR Journal*, 22 (3):27-42.

1 Introduction

The importance of evapotranspiration (ET) in the water cycle and hydrological management, in addition to the expensive and sensitive measuring equipments have

led to extensive efforts for modelling the ET process. Many methods have been developed, revised, and proposed with varied complexity levels for the estimation of ET in different climatic conditions using different predictor variables. ET is a complex and non-linear process since it depends on several interacting factors such as temperature, humidity, wind speed, radiation, and type and growth stage of crop (Jain et al., 2008; Bandyopadhyay and Bhadra et al., 2012; Adamala and Srivastava, 2018). Although there are many methods available for estimating reference evapotranspiration (ET_o), indirect methods of ET_o estimation are generally

Received date: 2019-05-22 **Accepted date:** 2019-08-26

*Corresponding author: Arnab Bandyopadhyay, Ph.D., Associate Professor, Department of Agricultural Engineering, North Eastern Regional Institute of Science and Technology, Nirjuli (Itanagar) – 791109, Arunachal Pradesh, India. Email: arnabbandy@yahoo.co.in. Tel: +919402275849, Fax: +913602258533.

used owing to cost, time constraint, and difficulty in measurement (Rana and Katerji, 2000; Liou and Kar, 2014; Tomar, 2015; Abarikwu et al., 2019). Appropriate choice of ET_o estimation method must be selected based on data availability and climatic conditions as the requirement of data differs for each method. Even for the same method, the performance varies with the climatic conditions (Jensen et al., 1990; Yang, 2015). FAO56-PM method (Allen et al., 1998) has been recognized as the standard method for indirect estimation of ET_o and for evaluating other methods (Allen et al., 2005) when comprehensive data are available (Mohammadigolafshani and Koulaian, 2018). Under limited data availability condition, Hargreaves method has shown reasonable ET_o estimates with global validity (Allen et al., 1998; Droogers and Allen, 2002). Crop ET (ET_c) is obtained from reference ET from a standard surface by multiplying with appropriate crop coefficient (k_c).

Irrigation for crop production is the largest consumptive user of fresh water accounting for more than 70% of global water withdrawal although irrigation is practiced only on 17% of total arable land (Xing et al., 2018). Continuous increase in water scarcity worldwide necessitates adopting efficient irrigation practices highlighting the importance of accurate estimation of net irrigation requirement (NIR) (Adeyemi et al., 2017). NIR, if known accurately can improve crop productivity and quality by applying the required amount in appropriate interval of time (Bhadra et al., 2012) and as spatially uniformly as possible. Efficient and effective water management strategies are essential for meeting the increasing water needs of agricultural, domestic, industrial, and environmental sectors.

The decision support system (DSS_ET) developed by George et al. (2002) supported nine widely used methods of ET_o estimation and later on, it was improved by Bandyopadhyay and Bhadra et al. (2012) which supported 22 ET_o estimation methods. This tool gives ET_o at point locations. DSS_ET was further linked with Arc DSS_ET by Bandyopadhyay and Mahendra et al. (2012) which is capable of reading five days forecasted data from India Meteorological Department (IMD) website for 75 stations. Although DSS_ET and Arc DSS_ET can

estimate ET_o at point locations, they lack the functionality to estimate the same in raster based approach. Furthermore, direct interpolation of point ET_o to generate ET_o raster produced inferior results as compared with ET_o raster generated using individually interpolated meteorological parameters (Hodam et al., 2017).

In the past years, different methods have been developed and used to estimate ET from remote sensing data (Tsouni et al., 2008; Cristobal et al., 2011; Liou and Kar, 2014). Remote sensing approaches though provide high spatial resolution and coverage, its temporal resolution is limited by the satellite revisit time and atmospheric conditions. These approaches cannot provide ET estimates under the possible future change of either individual climate factor or the land surface characteristics (Li et al., 2003). Moreover, only instantaneous estimates of ET can be obtained and it is difficult to derive daily values from a split second observation. In addition to that, besides being expensive, there is a need to analyse many images for seasonal ET estimates (Kite and Droogers, 2000).

GIS provides a powerful tool for integrating and processing large amounts of spatially distributed data such as the environmental variables needed to evaluate water balance terms. Many GIS tools and toolbar have been developed for modelling ET . A grid based toolbar (ArcET) developed by Li et al. (2003) uses ArcObjects for the purpose of regional ET modelling. This toolbar estimates ET from ground meteorological data with available land cover information through the conventional reference ET – crop coefficient approach. An ArcGIS toolbar rGIS-ET (Shu et al., 2006) uses LANDSAT data and MODIS data for estimating regional ET and was used to demonstrate its utility for estimating ET and evaluating agriculture water resource usage. Espana et al. (2011) developed a GIS tool (ArcE) in a vector based approach which uses ArcObjects using Hargreaves method for estimating potential ET and Budyko method for actual ET in monthly time steps from daily precipitation and temperature data. Despite the fact that ArcET, rGIS-ET, and ArcE can be used to estimate ET (in a raster based approach in the case of the former two and vector based approach in the latter), they lack the interface to estimate

NIR which is a function of ET_c and effective rainfall. Hence, there is a need to incorporate additional features to estimate both ET and NIR in raster based approach within a single framework to facilitate irrigation scheduling.

Raster data are preferred over vector data for some operations because of its ability to represent continuous surfaces and to perform surface analysis. Moreover, it can perform fast overlays with complex datasets which aids in visualization and interpretation. Nowadays, with the advancement in satellite technologies, an increasing amount of high spatial and temporal resolutions meteorological data are available as raster layers (Rathjens and Oppelt, 2012). Even IMD has started giving meteorological data as interpolated rasters. This study is an effort to develop a toolbar using ESRI ArcGIS ArcObjects in raster based approach to estimate ET as well as NIR within one toolbar. Integrating the two within one toolbar makes it easier for the user to perform ET and NIR analysis in one session making it more functional and user friendly. Average monthly ET_o and NIR maps

are generated directly from the toolbar through sequential calculation which could obviate the need for user to do spatial interpolation using geostatistical techniques to generate the same in case of vector based approach. This resulted in reduction in processing intensiveness and ultimately led to time saving.

2 Development of the toolbar

The toolbar was designed with the help of ArcObjects in ArcGIS platform. ArcObjects are a set of computer objects specifically designed for programming with ArcGIS Desktop applications (Burke, 2003; Law and Collins, 2018). It includes things like data frames, layers, features, tables, cartographic symbols, and the pieces that make up these things, namely points, lines, polygons, records, fields, colors and so on. ArcObjects incorporates all the functions of ArcGIS (ESRI, 2004) which permit any spatially distributed variables, such as, ET and NIR to be manipulated through the application programming interfaces.

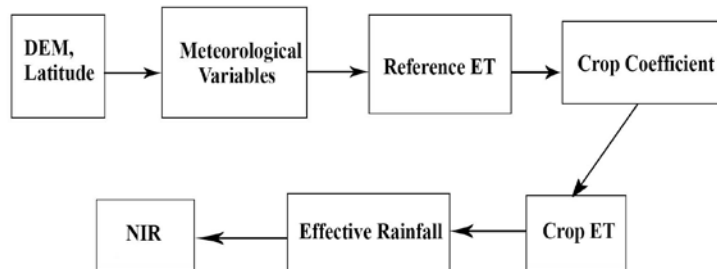


Figure 1 Framework for modelling ET and NIR in raster based approach

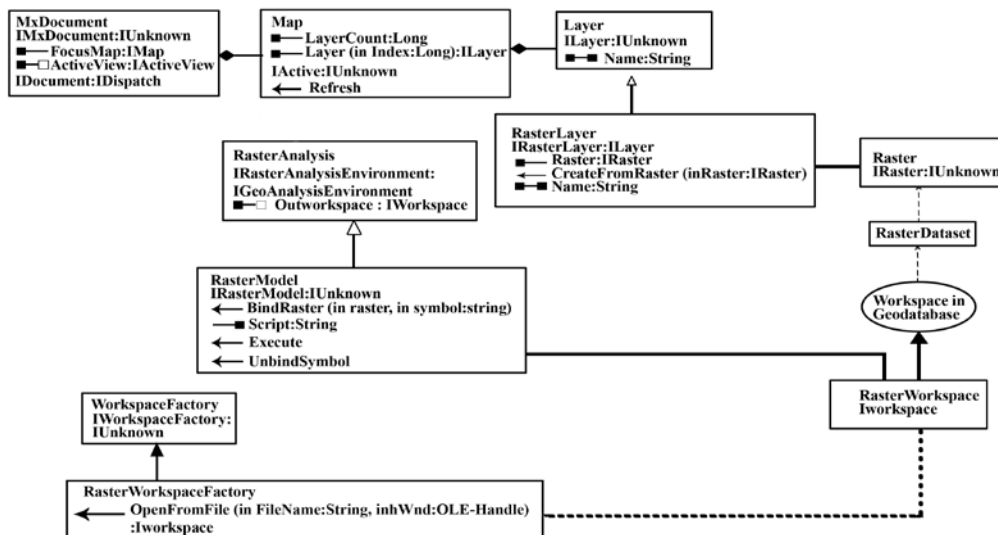


Figure 2 ArcObjects used in toolbar development



Figure 3 Interface used to estimate ET and NIR.

The framework of the raster based approach for ET and NIR modelling is shown in Figure 1. The important Arcobjects, programming interfaces, properties and methods used in implementing the toolbar is shown in Figure 2. The developed toolbar consists of 12 buttons (Figure 3). Out of which 9 buttons namely Save, Add Data, Full Extent, Zoom In, Zoom Out, Pan, Data View, Layout View, and Print are standard ArcGIS tools and the remaining 3 buttons namely ET_o , NIR and Help buttons were developed by the authors.

The toolbar can estimate ET_o on a daily or monthly basis depending on the input data supplied by the user either with Hargreaves and Samani or FAO56-PM method and calculate corresponding NIR on a monthly basis. The toolbar has the functionality to handle input data with different spatial resolutions. The resolution of the output rasters (ET and NIR layers) will be the coarsest resolution of the supplied input rasters. For input rasters with different spatial resolution, the final output raster is based on the resampling technique specified by the user in the environment setting of ArcGIS. Unless otherwise stated, nearest neighbour resampling technique is used. The spatial extent of the output will be the overlapping areas of all the layers involved in calculation. The units used in the toolbar are $^{\circ}C$ for temperature, $m\ s^{-1}$ for wind speed, % for mean relative humidity, $W\ m^{-2}$ for solar radiation, mm for rainfall, $^{\circ}$ for latitude, and m for elevation. In the toolbar, accumulated monthly rainfall is supplied as rainfall raster. ET_o and NIR are calculated in $mm\ d^{-1}$.

2.1 Calculation of ET_o

In this study, ET_o is calculated based on two methods namely Hargreaves and Samani method and FAO56-PM method. Several improvements over the original Hargreaves (1975) equation was proposed by Hargreaves and Samani (1982, 1985) for estimating grass-reference ET . In places where meteorological measurements are scarce, Hargreaves and Samani method is recommended for estimating ET_o (Heydari and Heydari, 2014; Cobaner

et al., 2016). Since solar radiation (R_s) data are not routinely available everywhere, Hargreaves and Samani proposed estimating R_s from extraterrestrial radiation, R_a , and form the following equation.

$$ET_o = 0.0023 \times \frac{1}{\lambda} \times R_a \times \sqrt{TD} \times (T_{mean} + 17.8) \quad (1)$$

Where, TD is the temperature difference between maximum and minimum temperatures, $^{\circ}C$; R_a is extraterrestrial solar radiation in $MJ\ m^{-2}\ d^{-1}$; T_{mean} is mean temperature, $^{\circ}C$; and λ is latent heat of vaporization at T_{mean} , $MJ\ kg^{-1}$.

Allen et al. (1998) simplified the basic Penman-Monteith equation by defining the reference crop as a hypothetical crop with an assumed height of 0.12 m ($h_c = 12\ cm$) having a surface resistance of $70\ s\ m^{-1}$ ($r_c = 70\ s\ m^{-1}$) and an albedo of 0.23, closely resembling the evaporation of an extensive surface of green grass of uniform height, actively growing, and adequately watered. With standardized height for wind speed, temperature and humidity measurements at 2.0 m, latent heat of vaporization (λ) = $2.45\ MJ\ kg^{-1}$, and specific gas constant (R) = $0.287\ kJ\ kg^{-1}\ ^{\circ}C^{-1}$. The FAO56-PM equation for daily time step is given below.

$$ET_o = \frac{0.408 \times \Delta \times (R_n - G) + \gamma \times \frac{900}{(T_{mean} + 273)} \times u_2 \times (e_z^o - e_z)}{\Delta + \lambda \times (1 + 0.34 \times u_2)} \quad (2)$$

Where e_z^o is saturation vapour pressure in kPa; e_z is actual vapour pressure in kPa; Δ is slope of saturation vapour pressure-temperature curve in $kPa\ ^{\circ}C^{-1}$; γ is psychrometric constant in $kPa\ ^{\circ}C^{-1}$; u_2 is wind speed at 2 m height in $m\ s^{-1}$; R_n is net radiation in $MJ\ m^{-2}\ d^{-1}$; and G is soil heat flux in $MJ\ m^{-2}\ d^{-1}$. G is assumed to be 0 for daily time step calculations.

For estimating ET_o using the toolbar, the first step is to input the raster data to the ArcGIS interface using the "Add Data" button provided in the toolbar. Clicking the "ET_o" button will open up the GUI which is shown in Figure 4. It allows the user to select the method to estimate ET_o either by Hargreaves and Samani method or FAO56-PM method. The user can select the appropriate method based on the data and suitability over the region. Once the method is selected, the data which are not required will be grayed out. The data required to estimate ET_o using Hargreaves and Samani method are latitude,

maximum temperature, and minimum temperature rasters while that of FAO56-PM method are latitude, elevation, maximum temperature, minimum temperature, mean relative humidity, wind speed, and solar radiation rasters. Day, month, and year for which ET_o is to be estimated is taken as an input from the user in “DD/MM/YYYY” format for daily ET_o estimation if daily input rasters are supplied. To estimate average ET_o of a month from monthly average input rasters, 15 is used as the day (“15/MM/YYYY”). Once the input raster layers are added, the combo boxes are populated with the layer names in the table of contents (TOC). From the drop down list of the combo boxes, appropriate layer is selected for each of the combo boxes. Clicking the “Calculate ET_o ” button will estimate ET_o based on the method selected and prompt the user where the generated ET_o layer will be saved. The ET_o layer so generated will get loaded on the TOC from where the user can save, print, export or do further analysis as per the requirement.

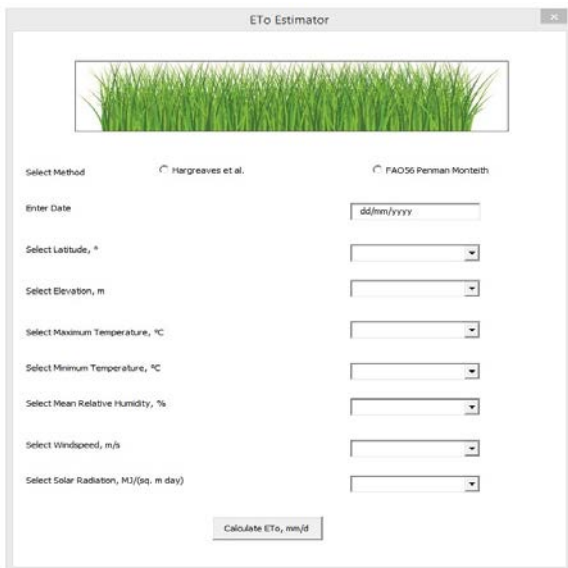


Figure 4 GUI for estimating ET_o

2.2 Calculation of NIR

For NIR calculation, the generated ET_o layer is multiplied by appropriate k_c values depending on the area-wise main crop grown in the respective agro-ecological region (AER) and its stage of growth in a particular month to get monthly ET_c raster.

$$ET_c = ET_o \times k_c \tag{3}$$

The normal monthly total rainfall values were converted into effective rainfall using the following relationship presented by USDA Soil Conservation

Service (SCS, 1970) as given below. Soil profile water loses through evapotranspiration and deep percolation loses to the underlying groundwater is considered (Bos et al., 2008; Ali and Mubarak, 2017) in this equation.

$$R_e = (1.25 \times R_t^{0.824} - 2.93) \times (10^{0.000955ET_{cm}}) \tag{4}$$

R_e is monthly effective rainfall in mm; R_t is monthly total rainfall in mm; and ET_{cm} is monthly total crop ET in mm.

The monthly effective rainfall values are then deducted from corresponding monthly cumulative ET_c to determine the net monthly irrigation requirement.

$$NIR = ET_{cm} - R_e \tag{5}$$

Where NIR = Net irrigation requirement in mm.

The “NIR” button is used for estimating NIR on a monthly basis. The ET_o layers so generated using the toolbar are multiplied with appropriate k_c values to get crop ET. Monthly NIR is estimated by using the average monthly ET_c values by multiplying it with the number of days in that month to get monthly ET_c from which effective rainfall values are deducted. Clicking the “NIR” button will open up the window which is shown in Figure 5. The combo boxes are populated with all the layers’ name loaded on the TOC. User will select the appropriate layer name loaded for each of the three combo boxes. Clicking the “Calculate NIR” button will estimate the NIR and prompt the user where the generated layer will be stored on the computer and the generated layer will appear on the TOC from where the user can save, print, export or do further analysis.

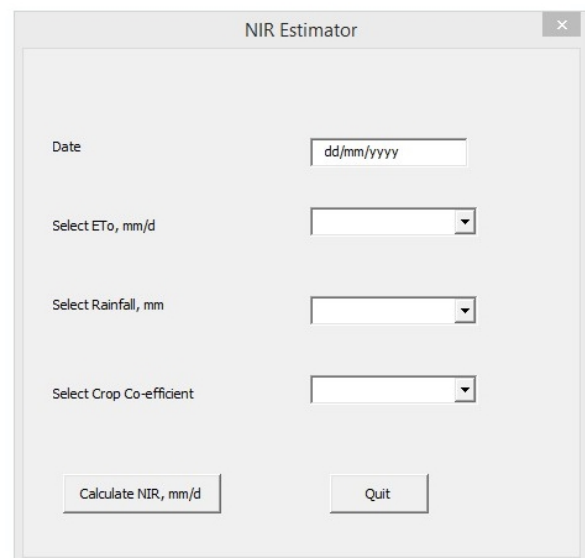


Figure 5 GUI for estimating NIR

3 Materials and methods

3.1 Study area and data acquisition

The toolbar was tested by implementing it for the whole India. The country lies in the northern hemisphere between 8°44' to 37°6' N latitude and 68°7' to 97°25' E longitude having a geographical area of 3,287,263 km². The average annual rainfall of the country is 1183 mm (Guhathakurta and Rajeevan, 2008). Of this, over 75% of it is received in the four rainy months of June to September only thereby leading to large variations on temporal scale (Kaur and Purohit, 2013). The study area comprises of 21 AERs with different physiography, soils, bioclimate, and the length of growing period.

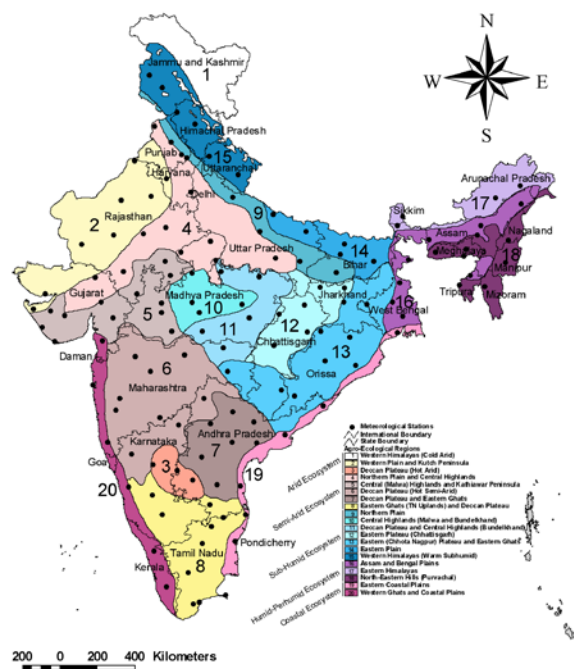


Figure 6 Agro-ecological regions of India and location of selected IMD stations

The elevation data was obtained from U.S. Geological Survey, EROS Data Center Distributed Active Archive Center (EDC DAAC) at a spatial resolution of 1 km. From the list of IMD meteorological stations, 133 stations were selected in such a way that they are evenly distributed across 19 AERs of India. Out of 21 AERs, two AERs namely, AER 21, i.e., Islands of Andaman-Nicobar and Lakshadweep and AER 1, i.e., Western Himalayas (Cold Arid) were excluded from the study due to spatial discontinuity and lack of data respectively. Monthly meteorological data (maximum and minimum air temperatures, relative humidity, wind speed, solar radiation, and rainfall) of these 133 stations for 30 years

(1971–2000) were procured from IMD. Normal monthly meteorological data were obtained by averaging the 30 years' data to test the toolbar. To obtain the spatial distribution of the stations within each of the 19 AERs, the AER map of India (Sehgal et al., 1990; Mandal et al., 2016) was digitized in Arcmap 10.1 and was overlaid on the point location of the stations. The spatial distribution of the selected stations within each of the 19 AERs is shown in Figure 6.

3.2 Preparation of input layers

Latitude layer was developed in geographic coordinate system and then projected it to the projected coordinate system. Twelve layers of normal monthly maximum temperatures, minimum temperatures, relative humidity, wind speed, solar radiation, and rainfall for twelve months (January–December) were prepared by spatial interpolation of point data collected from 133 IMD stations and were resampled at 1 km spatial resolution to match the spatial resolution of the elevation raster.

Spatial interpolation techniques, by which one can generate a surface from point data, are mainly of two types, viz., deterministic methods (e.g., inverse distance weighting method) and geostatistical methods (e.g., kriging). In deterministic methods, interpolated values are generated strictly from a neighbourhood of points based on a trend of values observed in the neighbourhood. Geostatistical methods, on the other hand, are more sophisticated and allow user to examine the spatial variability of data, statistical probabilities, and distance/directionality in generating the interpolated surface. The point meteorological data were interpolated using ordinary kriging method to generate the input rasters as suggested by Hodam et al. (2017).

The k_c raster for each month was prepared by analysing the cropping pattern of the country following Bhadra et al. (2012) (Table 1). To prevent the crops with higher water demand from facing water stress during their critical growth stages, the crop with the highest k_c of the month was selected if the growing periods of two or more main crops were found overlapping in some months while preparing the cropping pattern of the country. This will ensure meeting the water demand of the area-wise main crop with the calculated NIR since it is based on a crop

Table 2 Monthly k_c values in different agro-ecological regions

AER	Jan	Feb	Mar	Apr	May	Jun	Jul	Aug	Sep	Oct	Nov	Dec
AER 2	0.840	1.180	1.180	1.000	1.132	1.263	0.994	0.989	0.289	0.500	0.500	0.500
AER 3	1.061	1.000	1.043	1.086	0.518	1.000	1.115	1.231	0.476	1.000	1.030	1.061
AER 4	1.053	1.170	1.170	0.374	1.050	1.102	1.155	1.155	1.155	0.898	0.700	0.818
AER 5	1.195	0.383	1.000	1.029	1.087	1.144	1.173	1.173	0.579	0.700	0.947	1.195
AER 6	1.072	0.596	0.853	1.206	1.035	1.106	1.142	1.142	1.018	1.018	1.036	1.072
AER 7	1.127	1.205	1.205	0.766	1.000	1.039	1.117	1.156	1.154	1.154	1.154	1.050
AER 8	1.050	1.126	1.201	1.050	1.125	1.201	1.050	1.103	1.155	1.155	1.155	0.724
AER 9	1.135	1.135	1.044	1.088	0.508	1.050	1.092	1.133	1.133	0.713	0.700	0.917
AER 10	1.164	0.500	0.854	1.209	1.170	1.050	1.107	1.163	1.163	1.163	0.932	1.164
AER 11	1.051	0.500	0.853	1.205	1.161	1.050	1.098	1.146	1.146	1.146	1.026	1.051
AER 12	1.148	1.148	0.843	1.186	1.132	1.050	1.085	1.121	1.121	0.704	0.700	0.924
AER 13	1.134	1.217	1.217	1.050	1.101	1.152	1.152	1.134	1.134	1.134	0.881	1.050
AER 14	1.130	1.130	0.835	1.169	1.103	1.050	1.084	1.118	1.118	0.697	0.700	0.915
AER 15	1.029	1.139	1.139	0.329	1.000	1.059	1.117	1.140	1.140	0.743	0.700	0.810
AER 16	1.171	1.171	1.171	0.857	0.557	1.050	1.081	1.112	1.112	1.112	1.050	1.110
AER 17	1.113	0.706	1.000	1.046	1.091	0.341	1.000	0.991	0.982	1.000	1.057	1.113
AER 18	1.121	0.739	1.000	1.065	1.130	1.050	1.080	1.111	0.658	1.000	1.061	1.121
AER 19	1.111	1.173	1.173	0.746	1.000	1.065	1.130	1.130	1.150	1.150	1.150	1.050
AER 20	1.050	1.121	1.192	1.050	1.096	1.142	1.142	1.142	0.681	1.050	1.127	1.203

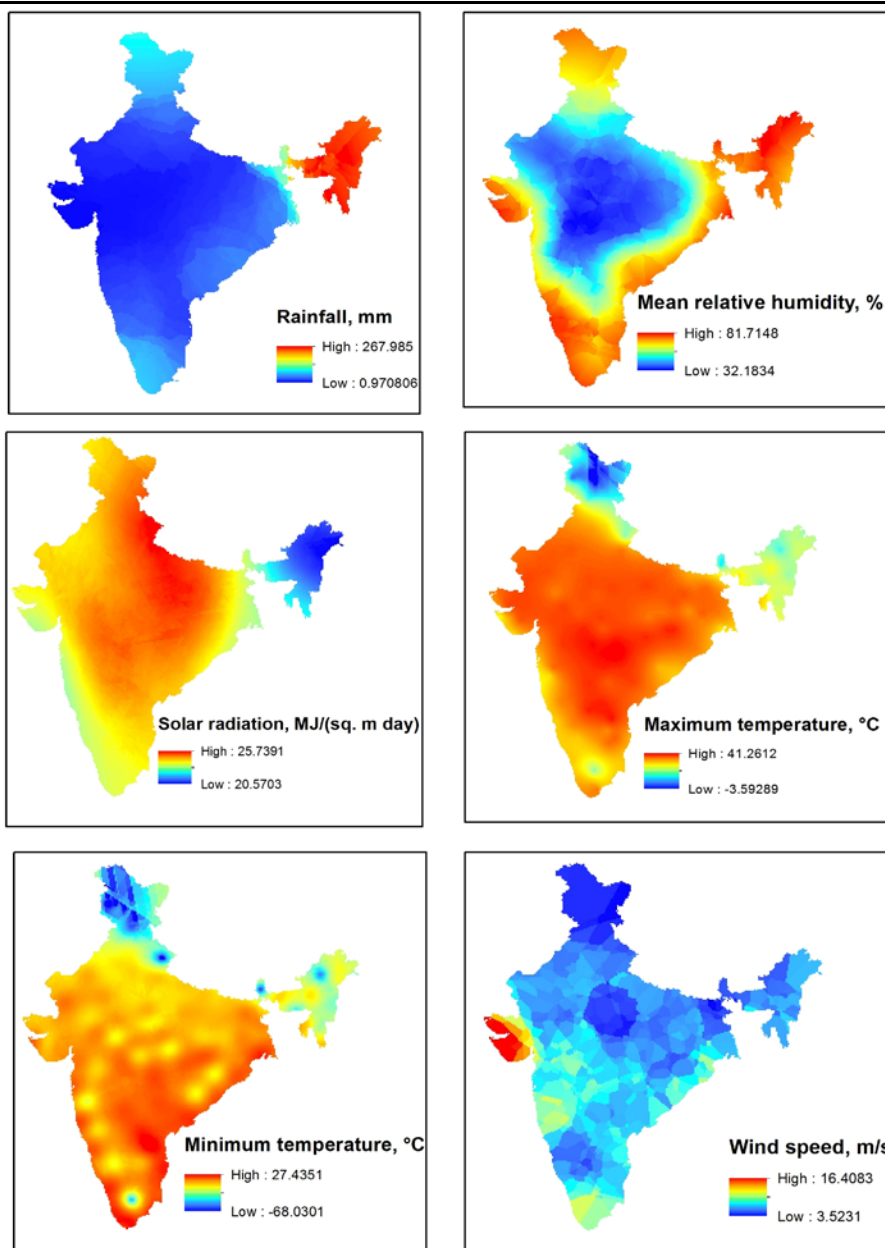


Figure 7 Input data for the month of May

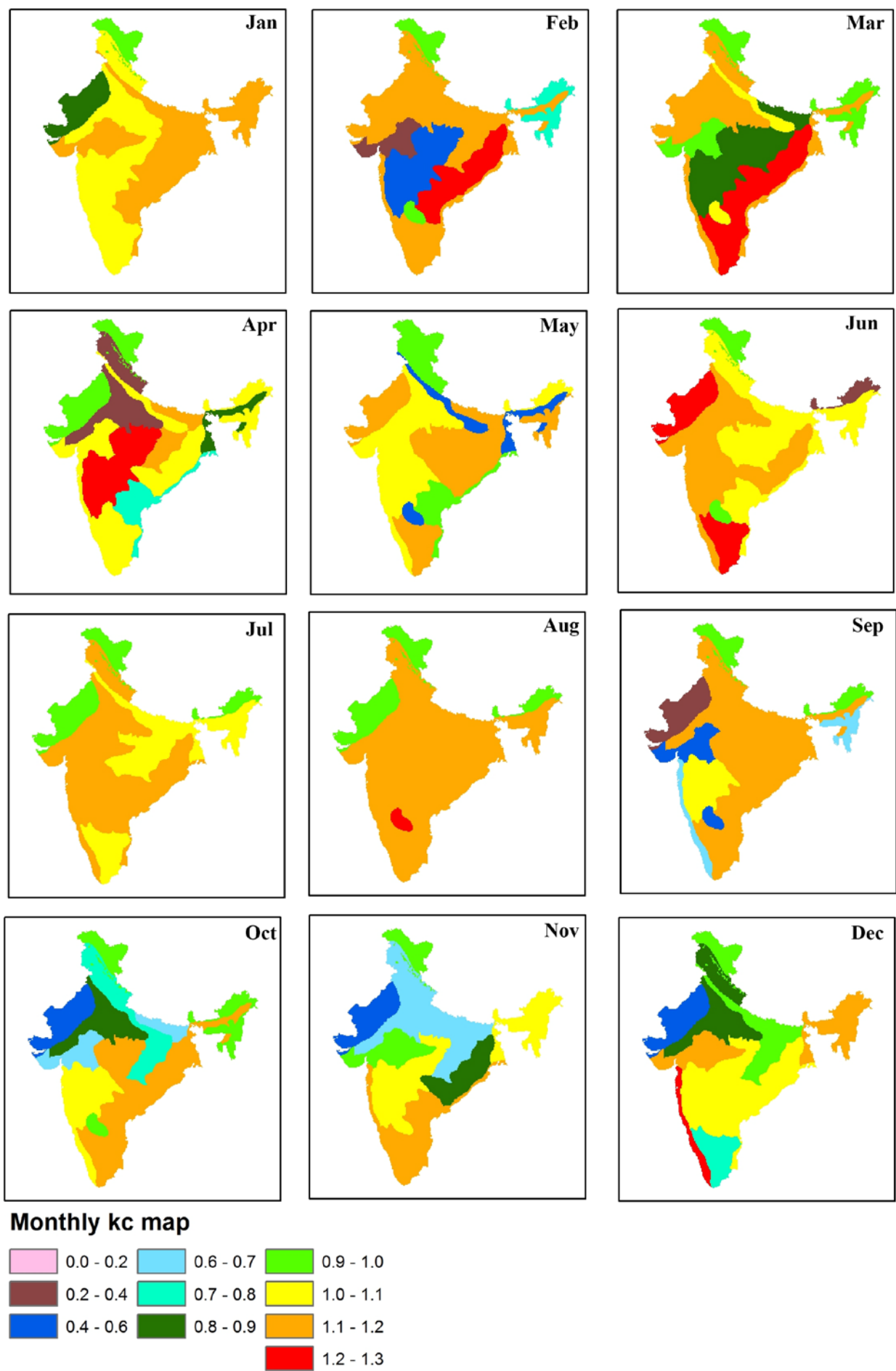


Figure 8 The k_c rasters for all the months

3.3 Estimation of ET_o and NIR

ET_o was estimated using the developed toolbar either with Hargreaves and Samani method (Equation 1) or FAO56-PM method (Equation 2) for each month and their corresponding NIR estimated using Equations 3–5. The required input layers for each method is mentioned in section 2.2. Despite utilizing only temperature data for estimating ET_o , Hargreaves and Samani method has proven to perform well (Sabziparvar and Tabari, 2010; Shahidian et al., 2012). The provision to estimate ET_o using Hargreaves and Samani method is provided for use in places where limited data are available.

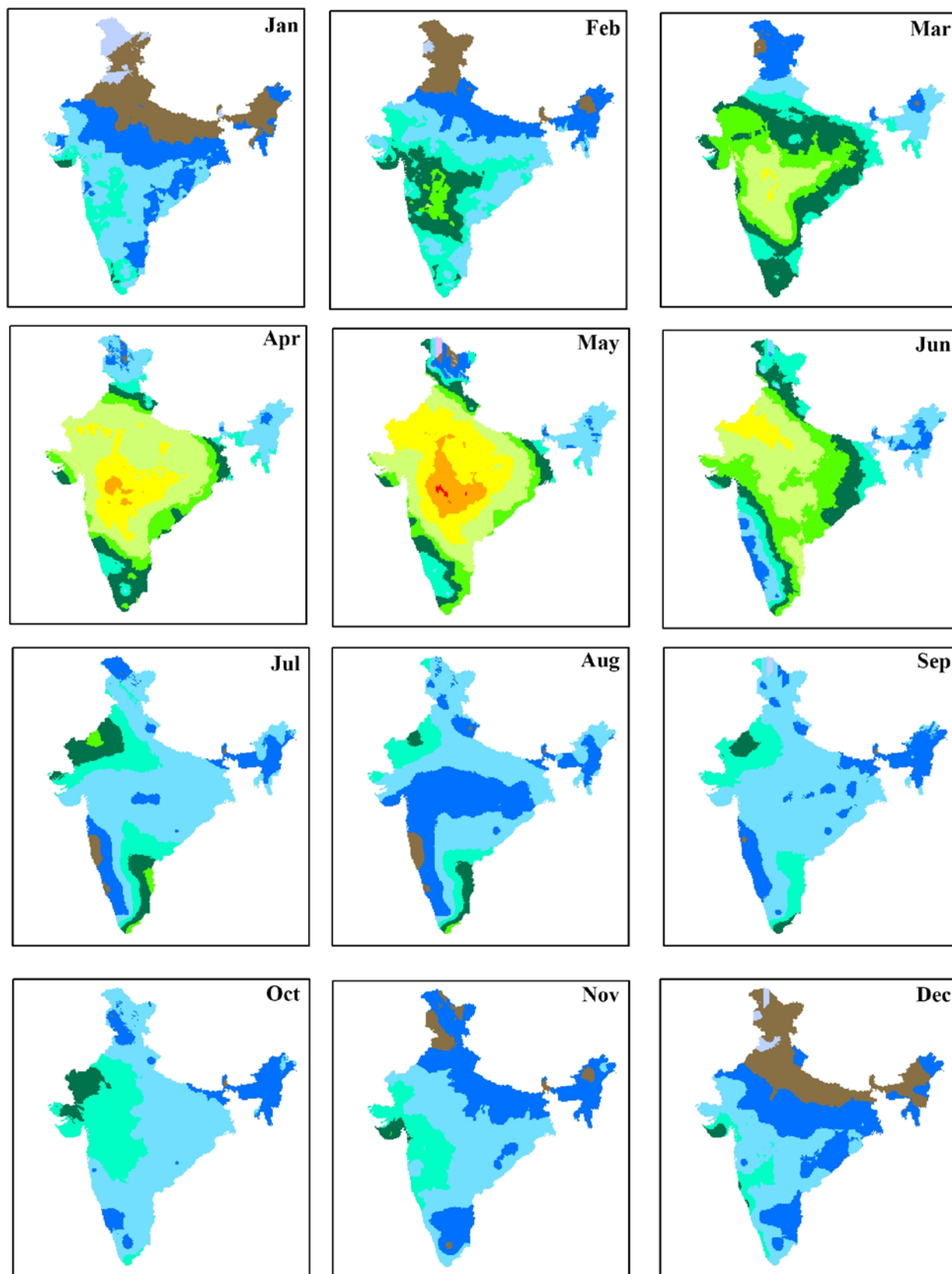
3.4 Verification of toolbar's calculation

The developed toolbar was verified using the monthly meteorological data of May for the year 2000. Average monthly ET_o and NIR layers generated for the month of May using the developed toolbar were extracted at ten evenly distributed locations. The verification points were chosen in such a way that they are distributed over different AERs. The values of input layers for the same month and year were also extracted at the same ten point locations using the Spatial Analyst Tools of ArcGIS. These extracted values were used to manually calculate the ET_o and NIR values at all the ten point locations for the month of May. These manually calculated values were then compared with the ET_o and NIR values extracted from raster layers generated by the developed toolbar.

4 Results and discussion

Using the developed toolbar, ET_o and NIR were estimated on a monthly basis. ET_o was estimated using both Hargreaves and Samani method and FAO56-PM method. ET_o and the corresponding NIR estimated using FAO56-PM method for all the months are shown in Figure 9 and Figure 10, respectively. Each sub-figure in Figures 9 and 10 shows average monthly ET_o and NIR respectively for each month (January – December) in mm d^{-1} . As can be seen from Figure 9, ET_o estimated using FAO56-PM method is highest in the month of May and

lowest in the month of October with a value of 7.7 mm d^{-1} and 4.6 mm d^{-1} respectively when averaged over the whole country. While using Hargreaves and Samani method, the highest and lowest ET_o values were obtained in the month of May and August respectively (Figure 11) with an area average value of 5.7 mm d^{-1} as the highest value and 4.2 mm d^{-1} as the lowest value. It can be seen that for all the months, ET_o estimated in the Western Himalayas, Eastern Himalayas, North Eastern Hills, and Northern Plain regions have relatively lower values as compared to the rest of the study area while ET_o values are relatively higher in the Central Highlands, Central Highlands and Kathiawar Peninsula, and Western Plain and Kutch Peninsula. NIR was estimated using the ET_o generated by using FAO56-PM method on a monthly basis and it was observed that the highest NIR value was obtained in the month of May (Figure 10) with an area average value of 5.9 mm d^{-1} and lowest area average value was obtained in the month of September (0.6 mm d^{-1}). NIR values remain relatively higher in the months of March, April and May as compared to other months which is expected because of extreme temperature, scarce precipitation, and long sunshine duration coupled with low relative humidity (Figure 10). Conversely, July, August, and September being part of monsoon season have relatively lower NIR when compared to other months as rainfall directly satisfies the crop water requirement (Figure 10). From Figure 10, it is clear that NIR which is a function of effective rainfall is closely related with the advancement and retreatment of monsoon. Northwest Rajasthan which is the last region to receive south-west monsoon in the Indian Peninsula shows higher crop water requirement in the month of June as compared with other areas. In this region, onset of monsoon takes place by mid-July while June remains dry. Likewise, Tamil Nadu which receives majority of its rainfall through north-east monsoon in the winter months of October, November, and December shows relatively lesser crop water requirements in these months as compared to other parts of India.



Monthly ET_0 , mm/d

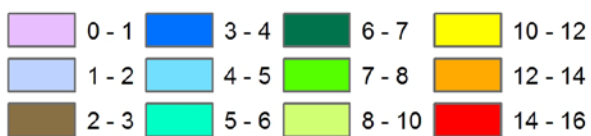
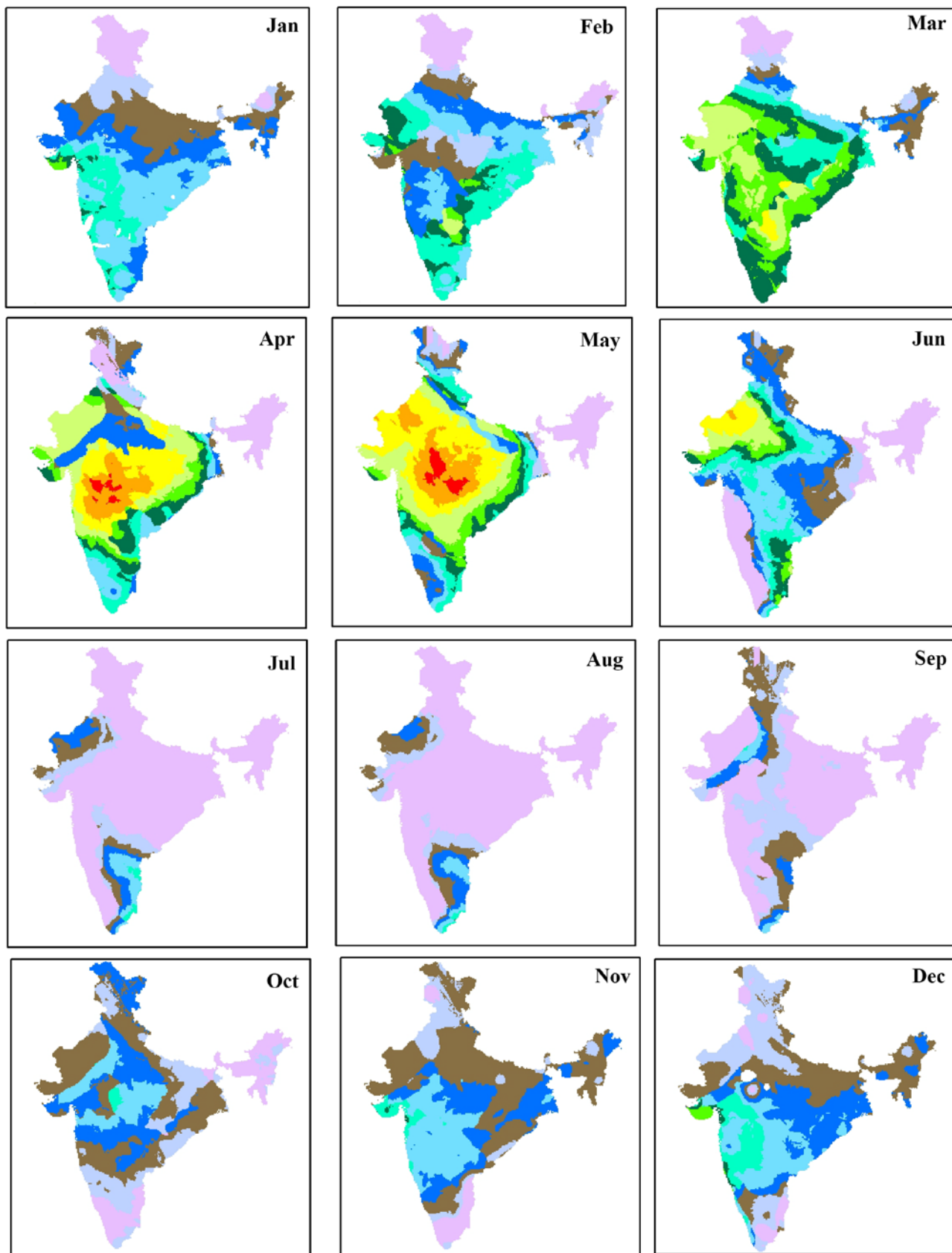


Figure 9 Monthly ET_0 , estimated using FAO56-PM method



Monthly NIR, mm/d

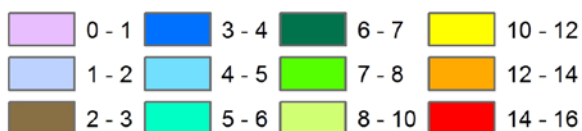


Figure 10 Monthly NIR estimated using monthly ET_o estimated by FAO56-PM method

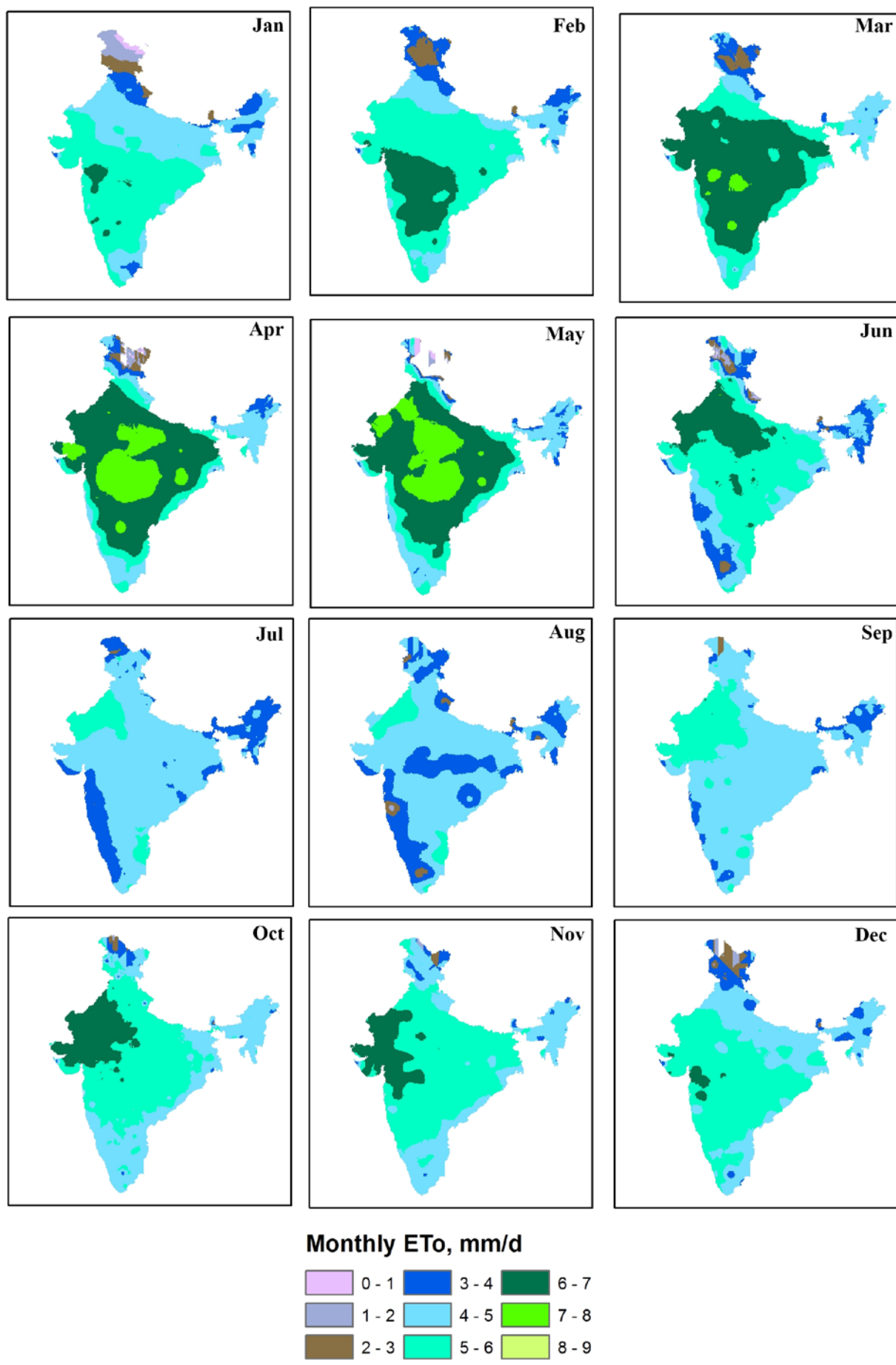


Figure 11 Monthly ET_0 estimated using Hargreaves and Samani method

The toolbar estimated ET_o and NIR values at ten evenly distributed locations were verified by comparing it with the manually calculated ET_o and NIR at the same locations for the month of May, 2000 as discussed earlier (Figure 12). For most of the verification points selected, ET_o exceeds NIR as is evident from Figure 12. But at some other locations where there is less rainfall coupled with high k_c values, NIR exceeds ET_o . It can be seen from the bar chart that the ET_o and NIR values generated by the toolbar are the same as that of the manually calculated ones. Hence, the developed toolbar was successfully verified and can be used to generate ET_o and NIR rasters when input data are available in raster formats.

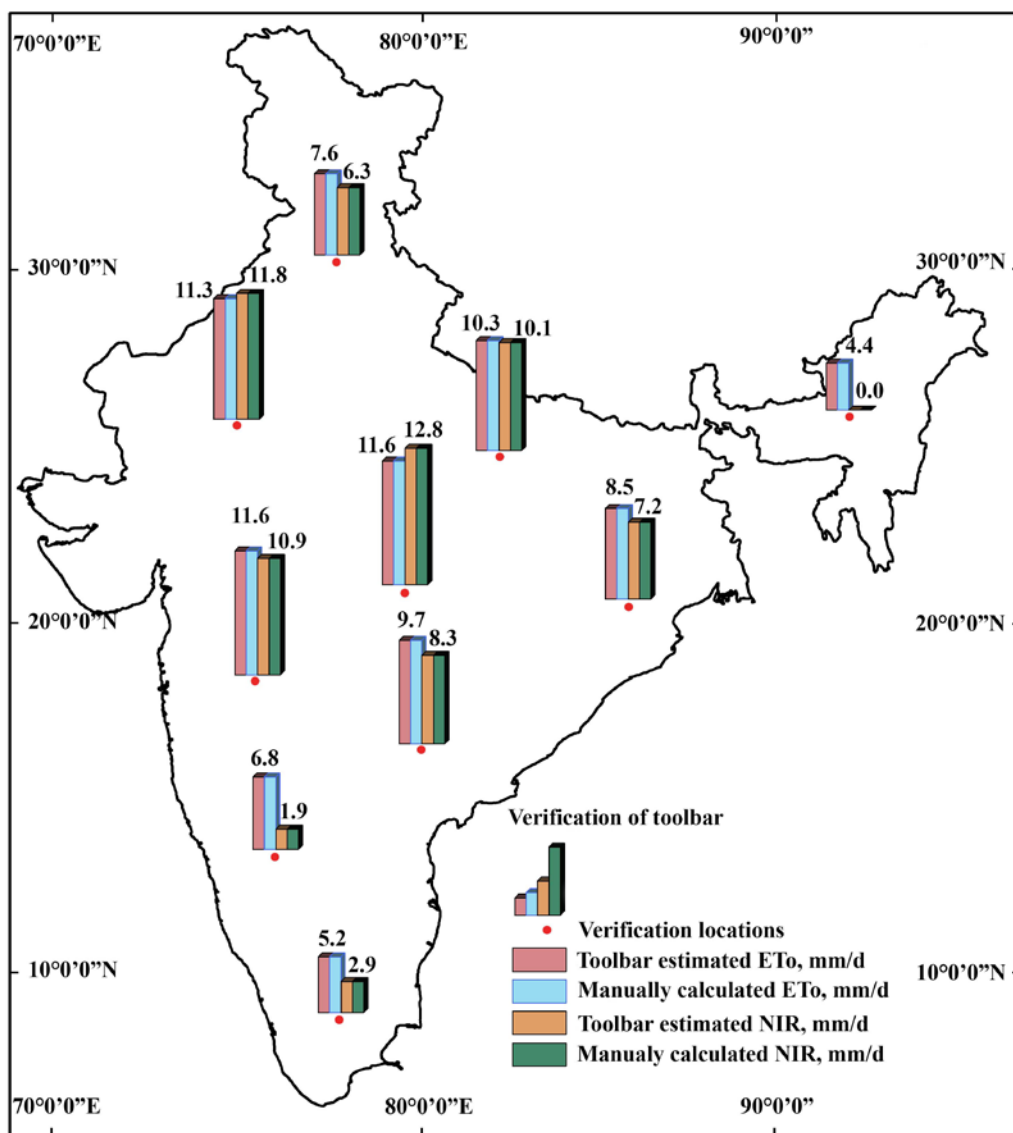


Figure 12 Verification of the developed toolbar at selected locations

5 Conclusions

The toolbar was designed with the help of ArcObjects in ArcGIS platform. It supports two methods of ET_o estimation either by Hargreaves and Samani method or FAO56-PM method. It can estimate daily ET_o or average monthly ET_o depending on the input rasters and gives average monthly NIR. To test the toolbar, twelve layers of normal monthly maximum temperatures, minimum temperatures, mean relative humidity, wind speed, solar radiation, and rainfall for all the months (January–

December) were prepared by spatial interpolation of point data collected from 133 IMD stations. The k_c rasters for each month were prepared by analysing the cropping pattern of the country (Bhadra et al., 2012). Using the developed toolbar, ET_o was estimated for all the twelve months with both the methods. NIR was estimated for all the months with the ET_o layers generated using FAO56-PM method. While area average ET_o estimated using FAO-56 PM method is highest in the month of May and lowest in the month of October, highest area average ET_o

value was obtained in the month of May and lowest in the month of August for ET_o estimated using Hargreaves and Samani method. Area average NIR was found to be highest in the month of May and least in the month of September. NIR values remain relatively higher in the months of March, April, and May as compared to other months which is expected because of extreme temperature, scarce precipitation, and long sunshine duration coupled with low relative humidity. July, August, and September being part of monsoon season have relatively lower NIR when compared to other months as rainfall directly satisfies the crop water requirement. NIR which is a function of effective rainfall is closely related with the advancement and retreatment of monsoon. The average monthly ET_o and NIR layers generated using the developed toolbar were verified at ten evenly distributed points by comparing it with the manually calculated ET_o and NIR values at those locations. It was found that the toolbar can generate accurate ET_o and NIR values and hence can serve as a handy tool for estimating crop water demand.

References

- Abarikwu, O. I., J. C. Adama, and E. U. Ezeani. 2019. Relationship between reference evapotranspiration and some climatic parameters, Umudike, Nigeria. *CIGR Journal*, 21(1): 28–33.
- Adamala, S., and A. Srivastava. 2018. Comparative evaluation of daily evapotranspiration using artificial neural network and variable infiltration capacity models. *CIGR Journal*, 20(1): 32–39.
- Adeyemi, O., I. Grove, S. Peets, and T. Norton. 2017. Advanced monitoring and management systems for improving sustainability in precision irrigation. *Sustainability*, 9(3): 353.
- Ali, M. H., and S. Mubarak. 2017. Effective rainfall calculation methods for field crops: an overview, analysis and new formulation. *Asian Research Journal of Agriculture*, 7(1): 1–12.
- Allen, R. G., L. S. Pereira, D. Raes, and M. Smith. 1998. Crop evapotranspiration – Guidelines for computing crop water requirements. In *Irrigation and Drainage Paper 56, Food and Agriculture Organization of the United Nations (FAO)*, 300. Rome, Italy: FAO.
- Allen, R. G., I. A. Walter, R. Elliott, T. Howell, D. Itenfisu, and M. Jensen. 2005. *The ASCE Standardized Reference Evapotranspiration Equation*. ASCE-EWRI, Reston, Virginia, 70p.
- Bandyopadhyay, A., A. Bhadra, R. K. Swarnakar, N. S. Raghuvanshi, and R. Singh. 2012. Estimation of reference evapotranspiration using a user-friendly decision support system: DSS_ET. *Agricultural and Forest Meteorology*, 154-155: 1–29.
- Bandyopadhyay, A., K. Mahendra, and N. S. Raghuvanshi. 2012. Forecasting daily net irrigation requirement maps of India using an ArcGIS toolbar. In *Sustainable Irrigation and Drainage IV*, ed. H. Bjornlund, section 3, 147–158. Southampton: WIT Press.
- Bhadra, A., N. S. Raghuvanshi, and R. Singh. 2012. Generation of monthly irrigation maps for India using spatial interpolation techniques. In *Sustainable Irrigation and Drainage IV*, ed. H. Bjornlund, section 5, 291–302. Southampton: WIT Press.
- Bos, M. G., R. A. L. Kselik, R. G. Allen, and D. J. Molden. 2008. *Water Requirements for Irrigation and the Environment*. Dordrecht: Springer.
- Burke, R. 2003. *Getting to Know ArcObjects*. Redlands, California: ESRI Press.
- Cobaner, M., H. Citakoglu, T. Haktanir, and O. Kisi. 2016. Modifying Hargreaves-Samani equation with meteorological variables for estimation of reference evapotranspiration in Turkey. *Hydrology Research*, 48(2): 480–497.
- Cristobal, J., R. Poyatos, M. Ninyerola, P. Llorens, and X. Pons. 2011. Combining remote sensing and GIS climate modelling to estimate daily forest evapotranspiration in a Mediterranean mountain area. *Hydrology and Earth System Sciences*, 15(5): 1563–1575.
- Droogers, P., and R. G. Allen. 2002. Estimating reference evapotranspiration under inaccurate data conditions. *Irrigation and Drainage Systems*, 16(1): 33–45.
- Espana, S., F. J. Alcalá, A. Vallejos, and A. Pulido-Bosch. 2011. ArcE: A GIS tool for modelling actual evapotranspiration. *Computers and Geosciences*, 37(9): 1468–1475.
- ESRI, 2004. *Geoprocessing in ArcGIS, Guide ArcGIS 9*. Redlands, California: ESRI Press.
- George, B. A., B. R. S. Reddy, N. S. Raghuvanshi, and W. W. Wallender. 2002. Decision support system for estimating reference evapotranspiration. *Journal of Irrigation and Drainage Engineering*, 128(1): 1–10.
- Guhathakurta, P., and M. Rajeevan. 2008. Trends in the rainfall pattern over India. *International Journal of Climatology*, 28(11): 1453–1468.
- Hargreaves, G. H., and Z. A. Samani. 1982. Estimating potential evapotranspiration. *Journal of the Irrigation and Drainage Division*, 108(3): 25–230.
- Hargreaves, G. H., and Z. A. Samani. 1985. Reference crop evapotranspiration from temperature. *Applied Engineering in Agriculture*, 1(2): 96–99.
- Hargreaves, G. H. 1975. Moisture availability and crop production.

- Transactions of the ASAE*, 18(5): 980–984.
- Heydari, M. M., and M. Heydari. 2014. Calibration of Hargreaves-Samani equation for estimating reference evapotranspiration in semiarid and arid regions. *Archives of Agronomy and Soil Science*, 60(5): 695–713.
- Hodam, S., S. Sarkar, A. G. R. Marak, A. Bandyopadhyay, and A. Bhadra. 2017. Spatial interpolation of reference evapotranspiration in India: comparison of IDW and kriging methods. *Journal of the Institution of Engineers (India): Series A*, 98(4): 511–524.
- Jain, S. K., P. C. Nayak, and K. P. Sudheer. 2008. Models for estimating evapotranspiration using artificial neural networks, and their physical interpretation. *Hydrological Processes*, 22(13): 2225–2234.
- Jensen, M. E., R. D. Burman, and R. G. Allen. 1990. *Evapotranspiration and Irrigation Water Requirements. ASCE Manual and Report on Engineering Practice No. 70*. New York: ASCE.
- Kaur, S., and M. K. Purohit. 2013. *Rainfall Statistics of India. ESSO/IMD/HS/R.F.REPORT/02(2014)/18*. Mausam Bhawan, Lodhi Road, New Delhi: Hydromet Division, IMD.
- Kite, G. W., and P. Droogers. 2000. Comparing evapotranspiration estimates from satellites, hydrological model and field data. *Journal of Hydrology*, 229(1): 3–18.
- Law, M., and A. Collins. 2018. *Getting To Know ArcGIS Desktop*. Redlands, California: ESRI Press.
- Li, S., D. Tarboton, and M. McKee. 2003. Development of an ArcMap toolbar for regional evapotranspiration modeling. In *Proc. 23rd ESRI International User Conference*. San Diego, California, 7–11 July.
- Liou, Y. A., and S. K. Kar. 2014. Evapotranspiration estimation with remote sensing and other various surface energy balance algorithms – a review. *Energies*, 7(5): 2821–2849.
- Mandal, D. K., C. Mandal, and S. K. Singh. 2016. *Agro-Ecological Regions of India (Revised), NBSS&LUP Publ. No 170*. Nagpur, India: ICAR-NBSS&LUP.
- Mohammadigolafshani, N., and A. Koulaian. 2018. Utilization of new computational intelligence methods to estimate daily evapotranspiration of wheat using gamma pre-processing. *CIGR Journal*, 20(3): 1–12.
- Rana, G., and N. Katerji. 2000. Measurement and estimation of actual evapotranspiration in the field under Mediterranean climate: a review. *European Journal of Agronomy*, 13(2-3): 125–53.
- Rathjens, H., and N. Oppelt. 2012. SWATgrid: an interface for setting up SWAT in a grid-based discretization scheme. *Computers and Geosciences*, 45: 161–167.
- Sabziparvar, A. A., and H. Tabari. 2010. Regional estimation of evapotranspiration in arid and semi-arid regions. *Journal of Irrigation and Drainage Engineering*, 136(10): 724–731.
- Soil Conservation Service (SCS). 1970. Irrigation water requirements, Technical Release 21(TR-21). Washington, D.C.: USDA.
- Sehgal, J. L., D. K. Mondal, C. Mondal, and S. Vadivelu. 1990. *Agro-ecological regions of India*. Nagpur, India: Tech. Bull., NBSS Pub. 24, National Bureau of Soil Survey and Land Use Planning (NBSS&LUP), Indian Council of Agricultural Research (ICAR).
- Shahidian, S., R. Serralheiro, J. Serrano, J. Teixeira, N. Haie, and F. Santos. 2012. Hargreaves and other reduced-set methods for calculating evapotranspiration. In *Evapotranspiration – Remote Sensing and Modeling*, ed. A. Irmak, ch. 4, 59–80. Rijeka, Croatia: InTech.
- Shu, Y., Y. Lei, L. Zheng, and H. Li. 2006. An evapotranspiration (ET) model based GIS using LANDSAT data and MODIS data with improved resolution. In *Proc. SPIE 6366, Remote Sensing for Environmental Monitoring, GIS applications, and Geology VI*, 63661N-1–63661N-10. Stockholm, Sweden, 11–14 September.
- Tomar, A. S. 2015. Development and comparative evaluation of radiation-based reference evapotranspiration equations for sub-humid Hazaribagh region of Jharkhand. *CIGR Journal*, 7(3): 10–20.
- Tsouni, A., C. Kontoes, D. Koutsoyiannis, P. Elias, and N. Mamassis. 2008. Estimation of actual evapotranspiration by remote sensing: application in Thessaly Plain, Greece. *Sensors*, 8(6): 3586–3600.
- Xing, W., W. Wang, Q. Shao, and Y. Ding. 2018. Estimating net irrigation requirements of winter wheat across central-eastern china under present and future climate scenarios. *Journal of Irrigation and Drainage Engineering*, 144(7): 05018005.
- Yang, Y. 2015. Comparison of dual-source evapotranspiration models in estimating potential evaporation and transpiration. In evapotranspiration over heterogeneous vegetated surfaces. Ph.D. diss., Berlin, Heidelberg: Springer.